Carbohydrate Polymers 82 (2010) 128–135

Contents lists available at ScienceDirect

Carbohydrate Polymers

journal homepage: www.elsevier.com/locate/carbpol

How does water diffuse in starch/montmorillonite nano-biocomposite materials?

Frédéric Chivrac[a], Hélène Angellier-Coussy[b], Valérie Guillard[b], Eric Pollet[a], Luc Avérous[a,*]

[a] LIPHT-ECPM, EAc(CNRS) 4379, Université de Strasbourg, 25 rue Becquerel, 67087, Strasbourg Cedex 2, France
[b] Unité Mixte de Recherche "Ingénierie des Agropolymères et Technologies Emergentes", INRA/ENSA.M/UMII/CIRAD, Université Montpellier II, CC023, place E. Bataillon, 34095, Montpellier Cedex, France

ARTICLE INFO

Article history:
Received 2 March 2010
Received in revised form 12 April 2010
Accepted 14 April 2010
Available online 24 April 2010

Keywords:
Starch
Nanocomposite
Water permeability

ABSTRACT

The objective of the paper is to examine in detail the relationship between the structure of starch-based nano-biocomposite materials (containing 0, 3 and 6 wt% of native sodium, and organo-modified montmorillonites with cationic starch) and their moisture barrier properties (permeability, water sorption and diffusivity). The structure was characterized by TEM, WAXD and DMA, whereas moisture transfer was evaluated thanks to permeability measurements and sorption kinetics analysis using a dynamic vapour sorption equipment. It was shown that the relatively high plasticizer content (23 wt% glycerol) induces a phase separation, with plasticizer rich and carbohydrate rich phases, resulting in the nanoclay being preferentially located in the carbohydrate rich domains. As a consequence, a preferential way for water transfer was more likely created in the very hydrophilic glycerol rich domains where the nanoclay platelets were almost totally absent. Thus, even if exfoliated morphology is achieved, the heterogeneous clay distribution and phase separation phenomena explain the lack of improvement and even the decline in the moisture barrier properties for these glycerol-plasticized starch nano-biocomposites.

1. Introduction

In the last decade, the increasing awareness concerning the human impact on the environment and the depletion of fossil resources have led to the development of efficient solutions to produce new environmentally friendly materials. Particular attention has been paid to the replacement of non-degradable petroleum-based plastics by materials based on biodegradable polymers from renewable resources, especially for packaging and disposable applications. Among these biopolymers, starch is considered as one of the most promising materials because of its large availability and relatively low price combined with its inherent biodegradability and renewable origin (Avérous, 2004). Several authors have already demonstrated the possibility to transform native starch into thermoplastic-like materials under destructuring and plasticizing conditions (Swanson, Shogren, Fanta, & Imam, 1993; Tomka, 1991). The most commonly used plasticizers for starch are water and polyols such as glycerol (Lourdin, Coignard, Bizot, & Colonna, 1997; Tomka, 1991; Van Soest, Dewit, Tournois, & Vliegenthart, 1994; Van Soest & Knooren, 1997). Despite their interesting mechanical properties, plasticized starch materials remain highly water sensitive with poor barrier properties and thus are not fully suitable for packaging applications (Gaudin, Lourdin, Forssell, & Colonna, 2000; Sorrentino, Gorrasi, & Vittoria, 2007).

The incorporation of nano-sized fillers into bio-based matrices, to produce nano-biocomposite materials, can be a powerful solution to improve these properties. Up to now, most of the studies have been focused on layered silicates, and especially on montmorillonite, as the reinforcing phase due to their large availability and versatility (Bordes, Pollet, & Avérous, 2009; Chivrac, Pollet, & Avérous, 2009). Compared to conventional composites, nanocomposites may display greatly improved properties, even at low nanofillers content (typically less than 5 wt%). Such improvement relies on the large interface area leading to the possibility of strong interactions between the polymer matrix and the nanofillers (Alexandre & Dubois, 2000; Bordes et al., 2009; Chivrac et al., 2009; Ray & Okamoto, 2003). Depending on the blending process conditions and on the polymer/nanofiller affinity, the layered silicates dispersed into the polymer matrix can be intercalated by polymer chains and/or exfoliated. The best performances are commonly observed for exfoliated structures in which the clay layers are individually delaminated and fully dispersed within the polymer matrix. Indeed, due to their high aspect ratio, small particle size and extremely large surface areas, the exfoliated clay platelets greatly increase the tortuous path for small diffusing molecules and thus can significantly improve the polymer gas and water barrier properties (Gorrasi et al., 2003; Sorrentino et al., 2007). It is thus of great importance to have a good polarity matching between the nanoclay surface and the matrix. That is why organo-modified montmorillonites are often used with hydrophobic synthetic polymers whereas the native sodium montmorillonite is preferred for polysaccharides such as starch and plasticized starch matrices

* Corresponding author. Tel.: +33 368852784; fax: +33 368852716.
E-mail address: luc.averous@unistra.fr (L. Avérous).

0144-8617/$ – see front matter © 2010 Published by Elsevier Ltd.
doi:10.1016/j.carbpol.2010.04.036

(Bordes et al., 2009; Chivrac, Pollet, Schmutz, & Avérous, 2008).

Many authors have already published on plasticized starch nano-biocomposites without obtaining a high extent of exfoliation (Chivrac et al., 2009). Indeed, commercial organo-modified montmorillonites do not match the starch hydrophilic character leading to poorly intercalated systems. For the hydrophilic sodium montmorillonite, it has been demonstrated that mainly glycerol preferential intercalation occurs, resulting in intercalated structures with a very low extent of exfoliation (Chivrac et al., 2008). Among these studies, several works were dedicated to water transport behaviour in glycerol-plasticized starch nano-biocomposites but all these works were performed on intercalated systems. More important, they led to inconsistent results with some authors claiming significant reduction in water permeability with the addition of clay whereas others observed unchanged or slightly increased water permeability (Cyras, Manfredi, Ton-That, & Vazquez, 2008; Mondragon, Mancilla, & Rodriguez-Gonzalez, 2008; Park, Lee, Park, Cho, & Ha, 2003; Tang, Alavi, & Herald, 2008a; Tang, Alavi, & Herald, 2008b; Zeppa, Gouanve, & Espuche, 2009).

Recently, some of us have demonstrated that the use of cationic starch as montmorillonite organo-modifier favours the clay exfoliation process into a plasticized starch matrix (Chivrac et al., 2008), leading to nano-biocomposites with markedly reinforced mechanical properties. It could be thus expected that moisture barrier properties will be also improved due to the increase of water diffusion pathway by the dispersion of the impermeable lamellae compared to the neat starchy matrix. However, little is known about the diffusional behaviour of water in such hybrid systems where the migrant (water) presents a high affinity for both the neat carbohydrate matrix and the nanoclays. It seems thus very important to clarify this point and improve knowledge about how does water diffuse in plasticized starch/montmorillonite nano-biocomposite materials.

The present work aims at improving the understanding of the relation between structure of nano-biocomposite materials based on plasticized starch and their moisture barrier properties (permeability, water sorption and diffusivity). The starch-based nano-biocomposites (containing 0, 3 and 6 wt% of native sodium, and organo-modified montmorillonites) were elaborated according to Chivrac et al. (2008). The structure was characterized by transmission electron microscopy (TEM), wide angle X-ray diffraction analysis (WAXD), and dynamic mechanical analysis (DMA). In order to assess the sorption kinetics, dynamic vapour sorption equipment was used. This gravimetric technique allows the continuous logging of weight changes at different equilibrating relative humidities at a specified temperature. The transient data of the sorption kinetics permit to identify a diffusivity value for each relative humidity level tested. The variations in water sorption, diffusivity and permeability were then related to the final structure obtained in the different tailored nano-biocomposites.

2. Materials and methods

2.1. Materials

Wheat starch was supplied by Roquette (France). The amylose and amylopectin contents were 23 and 77%, respectively. Residual protein content was less than 1%. The glycerol used as non-volatile plasticizer was supplied by the Société Française des Savons (France) and was a 99.5% purity product. The cationic starch was supplied by Roquette (France). Its charge density was 944 μequiv. g^{-1}. The cationic functions were quaternary ammonium with chloride as counter-anion. The Dellite® LVF sodium montmorillonite (MMT-Na) was supplied by Laviosa Chimica Mineraria S.p.A. (Italy) and presented a cationic exchange capacity (CEC) of 1050 μequiv. g^{-1}.

2.2. Samples preparation

2.2.1. Organo-modified montmorillonite preparation

The MMT-Na organo-modification was carried out with cationic starch using exfoliation/adsorption technique (Chivrac et al., 2008). 5 g of MMT-Na were introduced in 250 mL of distilled water and dispersed in ultra-sonic bath at 60 °C for 4 h. In parallel, 5.6 g of cationic starch were introduced in 250 mL of distilled water and solubilised in ultra-sonic bath at 60 °C for 1 h. These proportions corresponded to the charge equivalence between MMT and cationic starch. Then, the two solutions were pooled together and placed for 1 day at 60 °C in ultra-sonic bath. The solution was filtered and washed with 1 L of distilled water at 60 °C to remove the formed salt (NaCl) during the cationic starch adsorption. Then, the filtrate was lyophilized to obtain the cationic starch organo-modified montmorillonite (OMMT-CS).

2.2.2. Starch dry-blend preparation

The formulation used in this study contained 54 wt% of native starch, 23 wt% of glycerol and 23 wt% of water. Native wheat starch granules were first dried overnight at 70 °C in a ventilated oven to remove the free water (~10 wt% of the materials depending on the relative atmosphere humidity and temperature). Then, the starch powder was introduced into a turbo-mixer and the glycerol was slowly added under stirring. After complete addition of glycerol, the mixture was mixed at high speed (1700 rpm) to obtain a homogeneous dispersion. The mixture was then placed in a ventilated oven at 170 °C for 40 min and occasionally stirred, allowing vaporization of the bound water and diffusion of the glycerol into the starch granules. Such dry-blend protocol allows the preparation of plasticized starch with high glycerol content without exudation phenomenon, mainly thanks to the stronger interactions established between the polysaccharide chains and the glycerol plasticizer. To obtain the adequate moisture content, a determined quantity of water is added to this dry-blend after cooling and mixed at high speed (1700 rpm) (Avérous, Fringant, & Moro, 2001). The glycerol and water plasticized wheat starch (WS) dry-blend powder was then stored in a polyethylene bag.

2.2.3. Nano-biocomposites elaboration

To obtain nano-biocomposites, 3 and 6 wt% of nanoclay inorganic matter compared to the weight of starch and glycerol (1.38 and 2.86 g of clay inorganic fraction, respectively) have been added into the plasticized starch dry-blend. This mixture has been processed by mechanical kneading with a counter-rotating internal batch mixer, Rheocord 9000 (Haake, USA), at 70 °C for 20 min with a rotor speed of 150 rpm. After melt processing, moulded specimens and films were obtained by hot-pressing at 110 °C applying 20 MPa pressure for 15 min. The nano-biocomposite samples were then allowed to stabilize at 57% RH (relative humidity percentage) for 1 month in a controlled humidity chamber before characterization. Throughout this paper, the samples are designated WS/XXX *y*% where XXX stands for the type of nanoclay and *y* for the weight percentage of the inorganic clay fraction.

2.3. Characterization

2.3.1. X-ray diffraction analysis

The wide angle X-ray diffraction (WAXD) morphological analyses were performed on a powder diffractometer Siemens D5000 (Germany) using Cu (Kα) radiation (λ = 1.5406 Å) at room temperature in the range of 2θ = 10–30° by step of 0.01° of 4 s each.

Table 1
Bulk density (kg dry matter m^{-3} total matter) measured at 20 °C for native WS films and related nanocomposites.

Sample	Density
WS	1494 (61)
WS/MMT-Na 3 wt%	1474 (30)
WS/MMT-Na 6 wt%	1491 (44)
WS/OMMT-CS 3 wt%	1464 (58)
WS/OMMT-CS 6 wt%	1507 (42)

Values in brackets stand for the 95% confidence interval.

2.3.2. Transmission electron microscopy

For transmission electronic microscopy (TEM) observation, the samples were microtomed at low temperature (−80 °C) using a Diatome AG-microtome (Switzerland) equipped with a diamond knife. The ultra thin sections (nominal thickness 60 nm) were examined using a Philips CM 12 (Netherlands) transmission electron microscope using an acceleration voltage of 120 kV.

2.3.3. Dynamic mechanical analysis

Thermo-mechanical properties were determined using tensile geometry with a dynamic thermo-mechanical analyzer (TA Instrument DMA 2980, USA). Samples were cut to get specimens with dimensions 0.9 mm × 9.5 mm × 24.5 mm. The displacement amplitude was set to 15 μm. The measurements were performed at a frequency of 1 Hz. The range of temperature was from −70 °C to 70 °C at a scanning rate of 3 °C min^{-1}.

2.3.4. Water activity measurement

Water activity was measured at room temperature by using a FA-st lab device from GBX (France).

2.3.5. Density

The apparent density of the films was calculated at 20 °C from the ratio of the weight of dry matter (drying of films over P_2O_5) to the corresponding volume of total material (three replicates). Density values are given in Table 1.

2.3.6. Water vapour permeability measurements (WVP)

Water vapour permeability of the films was determined gravimetrically using a modified ASTM procedure (Gontard, 1991). The test film was sealed on the top of a permeation cell containing distilled water (100% RH; 2.337×10^3 Pa of vapour pressure at 20 °C), placed in a desiccator, and maintained at 20 °C (±0.1 °C) and 0% RH (0 Pa water vapour pressure) with silica gel. The water transferred through the film and adsorbed by the desiccant, was determined from the weight loss of the glass permeation cells. The cups were weighed daily to the nearest 0.1 mg. The slope of weight line compared with time was obtained by linear regression (correlation coefficients were 0.990 or greater). A minimum of five replicates for each film was measured. The measured water vapour permeability (WVP) of the film was determined as follows in the international system units:

$$WVP = \frac{w \cdot e}{A \cdot M \cdot (p_1 - p_2)} \quad (1)$$

where w is the slope of weight compared with time (kg s^{-1}), e is the film thickness measured after the WVP measurement (m), A is the area of exposed film (m^2), M is the molecular mass of water (kg mol^{-1}), and $p_1 - p_2$ is the vapour pressure difference across the film (Pa). As suggested by McHugh, Avenabustillos, and Krochta (1993), a correction of permeability values was done to take into account the external resistance to mass transfer. The thickness of the films was measured using a micrometer (Brave Instruments, Chécy, France) (10 replicates) in both the dry and hydrated states (at $a_w = 0.7$, just after water vapour measurement). The statistical significance of the experimental results was assessed using a single-factor analysis of variance (ANOVA). Multiple comparisons were performed by calculating the least significant difference. All tests were conducted at a 5% significance level.

2.3.7. Moisture sorption kinetic

Moisture sorption kinetics experiments were performed at 20 °C using a controlled atmosphere microbalance (Dynamic Vapour Sorption (DVS) apparatus; Surface Measurement System Ltd., London, UK) as previously described in the literature (Guillard, Broyart, Bonazzi, Guilbert, & Gontard, 2003; Roca, Broyart, Guillard, Guilbert, & Gontard, 2007). The DVS apparatus allows recording of mass evolution with time as a function of relative humidity of air. In practice, successive relative humidity steps (from 0 to 95%, with 10% step up to 90% and 5% step beyond) were performed for a same polymer sample and the remoistening kinetics was followed step by step until equilibrium between the carbohydrate material and surrounding atmosphere was reached. Moisture sorption isotherms were determined from the equilibrium moisture contents at each relative humidity step. Duplicates were done for each material tested.

2.3.8. Mathematical modelling of moisture sorption kinetic

The sample (diameter of 8 mm) used in the DVS apparatus was considered as a plane sheet with diameter to half thickness ratio superior to 80. Thus moisture transfer was considered one dimensional in the axial direction. The origin of the x-axis is placed at the interface between the air flux and the polymer surface. The mathematical model used in this study was the same than that developed and presented by Roca, Guillard, Broyart, Guilbert, and Gontard (2008) and validated on various porous and non-porous food materials and, notably, wheat gluten based films. This model supposes that the polymer is homogeneous and isotropic. It takes into account both the swelling of the polymer upon kinetics of water sorption by considering that the volume occupied by both water and dry matter is assumed to be equal to the sum of partial volume occupied by each phase (simplified deformation hypothesis) and the external resistance to mass transfer at the interface sample/surrounding atmosphere (h_m, in m s^{-1}). This external resistance expresses the resistance of diffusion through the mass transfer boundary layer for the vapour at the product surface (external resistance hypothesis). The external mass transfer coefficient was chosen equal to 8.165×10^{-3} m s^{-1} ($\pm 0.487 \times 10^{-3}$) as previously determined by Roca et al. (2007) for the geometry encountered in the DVS apparatus.

The mass conservation equation in the system can be modelled using the second Fick's law expressed in Lagrangian coordinate (fixed referential) in order to take into account the swelling of the sample during water sorption experiment written as:

$$\left(\frac{\partial X}{\partial t}\right) = \frac{\partial}{\partial \xi}\left(D^*_{eff}\frac{\partial X}{\partial \xi}\right) \quad \text{for} \quad 0 \le \xi \le \xi_{max}, \ \forall t \quad (2)$$

$$-D^*_{eff}\left(\frac{\partial X}{\partial \xi}\right) = 0 \quad \text{for} \quad \xi = 0, \ \forall t \quad (3)$$

where ξ and D^*_{eff} are respectively the Lagrangian coordinate (m) and modified apparent diffusivity (m^2 s^{-1}) calculated as follows:

$$D^*_{eff} = \frac{D_{eff}}{(1 + (\rho^0_{dm}/\rho^0_x)X)^2} \quad (4)$$

where D_{eff} stands for the effective diffusivity (m^2 s^{-1}) considered constant for a given relative humidity stage but variable from one stage to another, ρ^0_{dm} and ρ^0_x stand respectively for dry matter concentration in the binary mixture (kg m^{-3}) and water density (kg m^{-3}) and X is the moisture content (kg m^{-3}).

The boundary condition at $\xi = \xi_{max}$ is expressed as:

$$\frac{-\rho^0_{dm} D_{eff}(\partial X/\partial \xi)}{(1+(\rho^0_{dm}/\rho^0_x)X)^2} = \frac{h_m M}{RT} \quad (a_w p_{vsat} - p_{va}) \tag{5}$$

where M stands for the molar mass of water (18×10^{-3} kg mol^{-1}), p_{va} is the water vapour pressure in the surrounding atmosphere (Pa), p_{vsat} is the saturated water vapour pressure (Pa), R perfect gas constant (8.314 J mol^{-1} K^{-1}) and T is the temperature (K).

The Eulerian coordinate x_i corresponding to Lagrangian coordinate ξ_i is recalculated following:

$$x_i = \int_0^{\xi} \left(1 + \frac{\rho^0_{dm}}{\rho^0_x} X\right) d\xi \tag{6}$$

The system of Eqs. (2)–(5) was solved numerically as previously described in Roca et al. (2008) by using a specific algorithm developed in Matlab® and dedicated to the solving of this type of system of equations (corresponding Matlab® built-in function ode15s).

2.3.9. Moisture diffusivity identification

Constant values of effective moisture diffusivity at each relative humidity step were identified from experimental sorption kinetics by minimizing the root mean square deviations between simulated and experimental results using the Levenberg–Marquardt procedure (Gill, Murra, & Wright, 1981).

3. Results and discussion

3.1. Materials crystallinity upon ageing

Before studying barrier properties of the carbohydrate samples, it was of great importance to assess the crystallinity of the materials since this parameter may have an influence on the water transport results specially in plasticized wheat starch (WS) based films (Arvanitoyannis, Kalichevsky, Blanshard, & Psomiadou, 1994; Mali, Grossmann, Garcia, Martino, & Zaritzky, 2006). The wide angle X-ray diffraction (WAXD) patterns clearly showed an evolution upon ageing of the crystalline structure of WS-based materials stored at 57% RH and 20 °C for several weeks (Fig. 1(a)).

The diffraction pattern obtained for the plasticized unfilled matrix attested for a B-type crystalline structure with E_H-type crystallization peaks at 5.6° and 17.2°, corresponding to the amylopectin recrystallization. V_H-type crystallization peaks were also observed at $2\theta = 19.9°$ and 22.5° and corresponded to the process induced amylose crystallization into single helical structure (Van Soest, Hulleman, De Wit, & Vliegenthart, 1996a). This evolution is known for all starch gels (Katz, 1930). Upon ageing in humid atmosphere, the intensity of the peaks increased whereas their width decreased, revealing that both the crystallinity and the size of the crystallites increased. The major time evolution concerned the diffraction peak observed at ca. 17°, corresponding to a gradual increase in the amylopectin crystallization, which is a slow process. The two other main diffraction peaks were already present in the early stages of the material ageing and presented a rapid time evolution since the amylose crystallization occurred much faster. As a conclusion, these analyses showed that constant and stable properties were obtained after 1 month of ageing at 57% RH. The final degree of crystallinity depends on the capability of the chains to form crystallites and on the molecular mobility during re-crystallisation (Rindlav-Westling, Stading, Hermansson, & Gatenholm, 1998). According to the WAXD peaks area and to the data available from the literature for similar formulations (Van Soest, Hulleman, De Wit, & Vliegenthart, 1996b), the crystallinity was estimated to be around 10%.

Fig. 1(b) presents the WAXD patterns recorded after 1 month of ageing at 57% RH for WS-based materials and corresponding nanocomposites. All the nanocomposites samples display a B-type starch structure, as already observed for the unfilled matrix. Diffractograms clearly attest that the carbohydrates crystallinity was not affected by the addition of nanoclays since any evolution of the E_H-type and V_H-type crystallization peaks were observed for the starch nano-biocomposites samples. For all the samples, the crystallinity was very similar to the neat matrix and remained quite low.

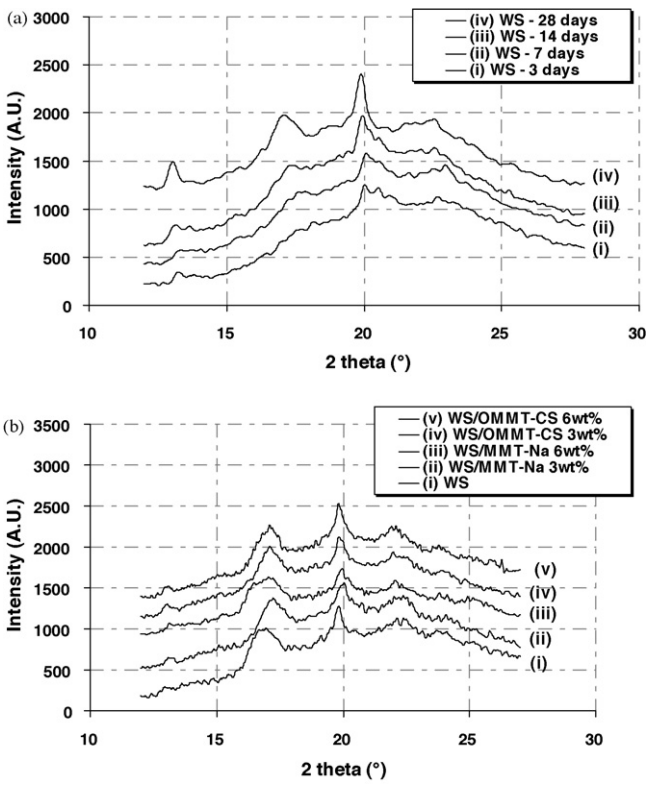

Fig. 1. WAXD patterns recorded for (a) non-aged and aged WS films upon post-processing ageing at 57% RH and (b) WS films and related nanocomposites after 28 days of ageing at 57% RH.

Thus, one can affirm that differences in water transport properties, if any, will only be related to the nanocomposite structure and not induced by variations in starch crystallinity.

3.2. Moisture transport properties

The effect of addition of native (MMT-Na) or modified (OMMT-CS) montmorillonite in WS-based films on their water sorption equilibrium and moisture diffusivity was first investigated.

3.2.1. Water sorption isotherm

The equilibrium moisture contents (EMC) of native WS, WS/MMT-Na 6 wt% and WS/OMMT-CS 6 wt% films at each tested water activity (a_w) were obtained from the water sorption kinetic profile. The corresponding plots of EMC vs. a_w (i.e., water sorption isotherms curves) are given in Fig. 2. The general aspect of the curve was the one observed for hydrophilic materials (Labuza, 1968). The EMC remained lower than 0.3 g g^{-1} dry basis (d.b.) for a_w lower than 0.7 and then sharply increased up to 1.0 g g^{-1} d.b. for high a_w values. These values were in accordance with those obtained by Enrione, Hill, and Mitchell (2007) on extruded wheat starch containing 20% of glycerol (EMC 0.43 g g^{-1} against 0.53 g g^{-1} d.b. in this study at 0.9 a_w). It should be emphasised that there are very few data available in literature concerning the water sorption behaviour of gelatinized wheat starch and WS-based biopolymers.

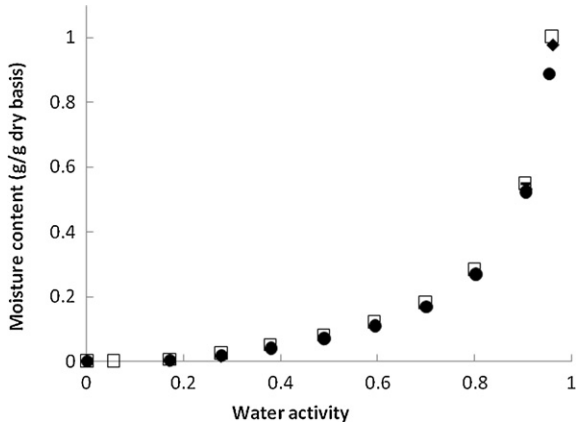

Fig. 2. Experimental water vapour sorption isotherm at 20 °C in WS (□), WS/MMT-Na 6 wt% (♦) and WS/OMMT-CS 6 wt% (●) films (vertical bars standing for the experimental error are too weak to be visible on the graph).

No significant effect of MMT addition on the EMC and, thus, the water sorption isotherm curves was noticed.

3.2.2. Apparent diffusivity of water

The apparent diffusivity of water in native WS, WS/MMT-Na 6 wt% and WS/OMMT-CS 6 wt% films were identified for each RH level from the water sorption kinetic curve measured using the DVS and by using the mathematical model developed. The diffusivity was assumed to be constant for each RH level and could change from one stage to another. It should be pointed out that the material swelled upon water sorption and that this swelling has been taken into account for a more accurate diffusivity determination. In such condition, the Fickian model used was not strictly representative of the various prevailing mechanisms of water transport in starch-based materials. The identified diffusion coefficient was thus considered as an apparent or effective diffusivity (called D_{eff}). The resultant D_{eff} values are plotted as a function of the average water activity of level for all the successive RH levels investigated (Fig. 3). A maximum D_{eff} value was observed at $a_w = 0.7$, where the equilibrium moisture content was 0.18 g g^{-1} d.b. This typical bell-like curve for D_{eff} values as a function of a_w is in agreement with other studies (Enrione et al., 2007; Hanson, Cramer, Abraham, & Lancaster, 1971; Karathanos, Villalobos, & Saravacos, 1990; Yu, Schmidt, Bello-Perez, & Schmidt, 2008). Yu et al. (2008), using the same method of water sorption kinetic than that used in this study, reported a maximum value of D_{eff} in dent corn starch granules (30% of crystallinity) at 0.5 a_w and significantly lower values for $a_w < 0.5$ and >0.5. Karathanos et al. (1990), using drying data, also noticed a maximum of diffusivity at intermediate moisture content in corn starch gels. Hanson et al. (1971), using the sorption kinetic technique, found that the diffusivity of water in individual corn starch granules reached a maximum near a moisture content of 0.15 g g^{-1} d.b. And finally, Enrione et al. (2007) using the same DVS system than that used in this study, found that D_{eff} in thermo-mecanically extruded wheat starch containing 20% of glycerol went by a maximum for an average a_w of 0.65. The bell-like curve for D_{eff} vs. a_w was also observed for other hydrophilic, porous products such as cereal-based products (Guillard et al., 2003; Roca et al., 2008). In most of the previous citations, this peculiar behaviour was believed to be due to a change in the mechanism of diffusion from vapour diffusion at low relative humidity to liquid diffusion at high relative humidity values related to the evolution of material's porosity with its moisture content. In the case of non-porous samples such as WS-based films, the low D_{eff} value obtained for $a_w < 0.4$ and then the increase in D_{eff} for $0.4 < a_w < 0.7$ could be related to the plasticizing effect of water which favours the movement of the carbohydrate polymer chains and then the diffusion of water molecules. The decrease in D_{eff} values for $a_w > 0.7$ in dense polymer such a starch-based materials was somewhere unexpected. Indeed, after a threshold value of a_w, plasticization of the polymer would not occur anymore and D_{eff} would stabilize to a plateau. It should be noted that in such hydrophilic material, the high amounts of water sorbed in the material for $a_w > 0.7$ could provoke additional phenomena such as polymer relaxation, which may induce a change in the diffusional mechanism as suggested previously by Enrione et al. (2007) to explain the unexpected decrease in diffusivity value for a_w above 0.6 in their extruded wheat starch. The Fickian model used to obtain D_{eff} would be not entirely appropriate to represent this different diffusional mechanism.

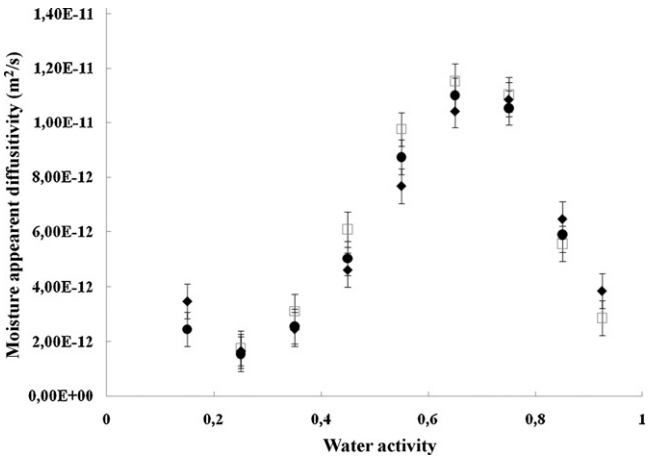

Fig. 3. Evolution of moisture apparent diffusivity at 20 °C in WS (□), WS/MMT-Na 6 wt% (♦) and WS/OMMT-CS 6 wt% (●) films (vertical bars stand for the experimental error on diffusivity determination).

The D_{eff} values found in this study varied from 0.15 to 1.18×10^{-11} m^2 s^{-1} and are in accordance with those found at 25 °C by Yu et al. (2008) in dent corn starch granules (varying from 0.9 to 2.0×10^{-11} m^2 s^{-1}) even though their sample were untransformed native granules.

The effect of MMT type on the moisture diffusivity value in WS matrix is not obvious in Fig. 3. Besides, MMT content had very little effect on the diffusivity value in WS/MMT nanocomposites compared to that obtained for the unfilled WS matrix (not shown here). However, a significant decrease in D value was obtained for WS/MMT-Na 6 wt% films for a water activity of 0.5 and 0.6 (decrease from 0.65 to 0.55×10^{-11} m^2 s^{-1} at $a_w = 0.5$ and from 1.0 to 0.7×10^{-11} m^2 s^{-1} at $a_w = 0.6$). As MMT content did not affect the water sorption equilibrium and little affected the water diffusivity, one may expect that the WVP of the WS nanocomposites materials will be very slightly decreased by the introduction of MMT compared to the WVP of the neat matrix.

3.2.3. Water vapour permeability

Water vapour permeability of native WS film and WS films filled with different contents of unmodified montmorillonite (MMT-Na) and organically modified montmorillonite (OMMT-CS) was tested for a 0–100% relative humidity (RH) difference (Table 2). Water vapour permeability (WVP) values are easier to determine than diffusivity and solubility ones and are, thus, commonly used to characterize the overall moisture barrier properties of polymers. The RH difference (0–100%) used in this study is the most common RH difference encountered in the literature and has thus been chosen in this work for easier comparisons with previous studies on similar carbohydrate biopolymers. With this RH difference, the average a_w of the films tested was 0.55. As expected, based on the previous analysis of diffusivity and sorption data obtained for

Table 2
Water vapour permeability (mol m^{-1} s^{-1} Pa^{-1}) at 20 °C for a relative humidity difference of 0–100% for native WS films and related nano-biocomposites.

Sample	WVP
WS	2.6 (0.21) × 10^{-11} a
WS/MMT-Na 3 wt%	2.7 (0.24) × 10^{-11} a,c
WS/MMT-Na 6 wt%	2.2 (0.45) × 10^{-11} b
WS/OMMT-CS 3 wt%	2.8 (0.15) × 10^{-11} a,c
WS/OMMT-CS 6 wt%	3.1 (0.32) × 10^{-11} c

Values in brackets stand for 95% confidence interval. WVP values with the same letter are not significantly different (single ANOVA + multiple comparison test).

these materials, the WVP values of the neat starch matrix and its related nanocomposites are very close and vary from 2.2 × 10^{-11} to 3.1 × 10^{-11} mol m^{-1} s^{-1} Pa^{-1} (Table 2). They were in the same order than values found for films prepared from pea starch (Zhang & Han, 2008) or potato starch (Rindlav-Westling et al., 1998). A precise comparison is difficult since water vapour transfers are strongly affected by various parameters such as the botanic origin of starch (Enrione et al., 2007), the respective content of amylose and amylopectin (Phan, Debeaufort, Luu, & Voilley, 2005; Rindlav-Westling et al., 1998), the crystallinity (Arvanitoyannis et al., 1994; Mali et al., 2006), the type and content of plasticizer (Enrione et al., 2007; Tang, Alavi, & Herald, 2008b; Zhang & Han, 2008) and the conditions of storage such as relative humidity (Phan et al., 2005).

The addition of nanoclays has a significant effect on WVP only for filler content of 6 wt% and for native MMT (MMT-Na) with a decrease of WVP from 2.6 to 2.2 × 10^{-11} mol m^{-1} s^{-1} Pa^{-1}. This result is totally in accordance with the results observed on sorption and diffusivity. The decrease of 1.2–1.4 order of magnitude in diffusivity values at a_w = 0.55 (average a_w value observed in samples used for measuring WVP) could explain the decrease in the WVP values (1.2-folds lower in presence of 6% MMT-Na in the WS matrix compared to the control) (Table 2). For the WS/OMMT-CS 6 wt% films, the WVP even tends to increase compared to materials with lower amounts of OMMT-CS. This tendency was not observed for the diffusivity value, which was not significantly different than that of the control and even tended to be lower.

The very low effect of the introduction of nanoclays on the moisture barrier properties of wheat starch-based nanocomposite films was unexpected for two main reasons. First, it was shown by some of us in a previous study that the OMMT-CS nanoclays were well exfoliated within the WS matrix since the X-ray diffraction patterns did not display the d_{001} diffraction peak characterizing the repetitive interlamellar distance (Chivrac et al., 2008). This was obtained by using cationic starch as the clay organo-modifier to tightly match the polarity of the carbohydrate matrix and thus to facilitate the clay exfoliation process. This exfoliation was confirmed by the TEM observations. It is known that an exfoliated morphology introduces a tortuous path for a diffusing penetrant. A reduction of permeability should arise from the longer diffusive path that the penetrant must travel in the presence of the layered silicates (Bharadwaj, 2001; Gorrasi et al., 2003). Secondly, some authors have already observed a permeability decrease of 2 orders of magnitude between unfilled WS-based materials and WS-based nano-biocomposite containing 10 wt% of natural montmorillonite (Tang et al., 2008a) and this was attributed to the exfoliated structure of the material.

In the present study, contrary to what was expected, the addition of MMT-Na and OMMT-CS in the WS matrix did not improve the moisture barrier properties of WS-based materials. In our case, the moisture barrier property of WS/OMMT-CS 6 wt% films was even exacerbated whereas the addition of OMMT-CS within the WS-based matrix was found to lead to a well-exfoliated morphology and to have a positive effect on the mechanical properties of the resulting nano-biocomposites (Chivrac et al., 2008). One

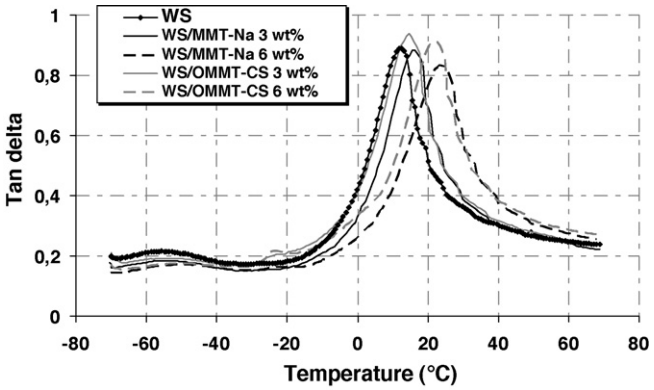

Fig. 4. tan δ curves for WS and related nanocomposites.

hypothesis that could explain this unexpected behaviour would be that a preferential pathway for water transfer is created in the WS matrix in specific domains where the layered silicates were completely or partially aggregated and non-exfoliated or even absent. In order to support this assumption, complementary studies were carried out using dynamic mechanical analysis (DMTA) and transmission electronic microscopy (TEM) to accurately determine the nano-structure of the WS/MMT-Na and WS/OMMT-CS nano-biocomposites.

3.3. Dynamic mechanical analysis and TEM observations

Thermo-mechanical measurements have been performed on WS-based nanocomposites to analyze the nanofiller dispersion state through its impact on the thermal properties. For all the studied systems, two relaxations peaks were observed on the tan δ curves (Fig. 4). The main relaxation (called α) is associated to the plasticized starch Tg. The second relaxation (called β), observed at lower temperature, is consistent with the plasticizer glass transition. For the sake of clarity, the T_α and T_β variations vs. clay content for glycerol-plasticized starch nano-biocomposites are reported in Table 3. The presence of these two relaxation peaks was related to the high glycerol content of the formulation, and could even reveal a phase separation between domains rich in carbohydrate chains and domains rich in plasticizer as previously hypothesized by Lourdin et al. (1997).

For T_β, only slight variations, which were not significant, were observed for all the samples tested. Such behaviour suggested that the nanoclays had no influence on the Tg of the domains rich in plasticizer. On the contrary, an important increase in the T_α with the clay content was observed for both nanoclays. At 3 wt% of clay loading, the nano-biocomposites prepared with both OMMT-CS and MMT-Na presented almost the same T_α. For higher clay content, the T_α values observed for MMT-Na were slightly higher than those obtained for the materials elaborated with OMMT-CS. Since the better the clay dispersion, the higher the clay/matrix interface area, a higher T_α was expected for the WS/OMMT-CS samples. This unexpected result could be explained by the morphology of the WS/MMT-Na films. Indeed, it was previously demonstrated that such nano-biocomposites displayed an intercalated structure with

Table 3
T_α and T_β values for native WS films and related nanocomposites.

	WS	WS/MMT-Na		WS/OMMT-CS	
Filler content (wt%)	0	3	6	3	6
T_α (°C)	11.7	15.7	23.9	14.9	21.7
T_β (°C)	−54.6	−54.9	−50.6	−53.6	−51.6

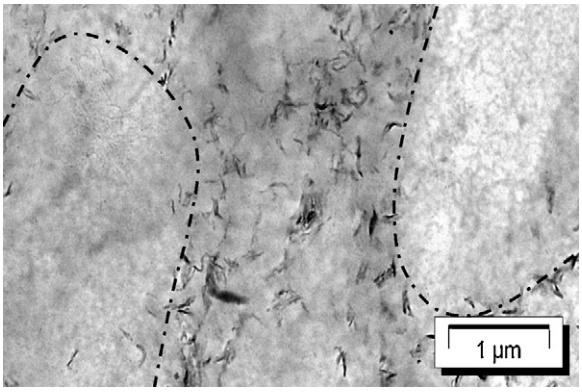

Fig. 5. TEM picture of WS/OMMT-CS 3 wt% highlighting the phase separation phenomenon.

preferential plasticizer intercalation (Chivrac et al., 2008). Consequently, a part of the plasticizer is confined into the galleries of clay platelets and cannot participate in the starch matrix plasticization, explaining the higher T_α obtained with MMT-Na compared to OMMT-CS. These results were also supported by the TEM observations where a phase separation between domains rich in clay platelets and domains without nanofillers was clearly observed (Fig. 5). As previously stated, such phase separation was likely induced by the use of a high glycerol content in the formulation.

According to the thermo-mechanical analyses, only T_α was influenced by the addition of nanoclays and shifted to higher temperatures. This result demonstrated that the clay platelets were preferentially located in the domains rich in carbohydrate chains. As a consequence, a preferential way for water transfer was more likely created in the specific domains where the layered silicates were almost totally absent. In addition, these domains without nanoclays should present a very hydrophilic character due to their high glycerol content. Thus, even if an exfoliated morphology is achieved with OMMT-CS (Chivrac et al., 2008), the heterogeneous clay distribution and phase separation phenomena explain the lack of improvement and even the decline in the moisture barrier properties for these glycerol-plasticized starch nano-biocomposites.

4. Conclusion

Contrary to what was expected, the addition of native sodium montmorillonite (MMT-Na) or montmorillonite modified with cationic starch (OMMT-CS) did not improve the moisture barrier properties of glycerol-plasticized wheat starch materials. In our case, the moisture barrier property of WS/OMMT-CS 6 wt% films was even exacerbated whereas it was found that OMMT-CS nanoparticles were well exfoliated within the starch matrix.

Since no change in crystallinity of the starch-based matrix was observed with the introduction of montmorillonites, this unexpected behaviour was rather explained by the fact that a preferential pathway for water transfer was created in the matrix. This assumption was supported by TEM and DMA analyses that both clearly demonstrated that the clay platelets were preferentially located in the domains rich in polysaccharide chains as a result of a phase separation. The preferential way for water transfer was more likely created in the specific glycerol rich domains where the layered silicates were almost totally absent and that present a very hydrophilic character due to their high glycerol content. Thus, even if an exfoliated morphology is achieved with OMMT-CS, the heterogeneous clay distribution and phase separation phenomena explain the lack of improvement and even the decline in the moisture barrier properties for these glycerol-plasticized starch nano-biocomposites.

In a recent publication (Chivrac, Pollet, Dole, & Avérous, 2010), some of us have shown that the nano-structure of starch-based nano-biocomposites strongly depends on the plasticizer type. Thus, the perspective of this work could be to analyse the impact of other less conventional plasticizers, such as, e.g., sorbitol which is solid at room temperature, on the permeability behaviour of the corresponding starch-based nano-biocomposites.

References

Alexandre, M., & Dubois, P. (2000). Polymer-layered silicate nanocomposites: Preparation, properties and uses of a new class of materials. *Materials Science & Engineering R-Reports*, *28*(1–2), 1–63.

Arvanitoyannis, I., Kalichevsky, M., Blanshard, J. M. V., & Psomiadou, E. (1994). Study of diffusion and permeation of gases in undrawn and uniaxially drawn films made from potato and rice starch conditioned at different relative humidities. *Carbohydrate Polymers*, *24*(1), 1–15.

Avérous, L. (2004). Biodegradable multiphase systems based on plasticized starch: A review. *Journal of Macromolecular Science-Polymer Reviews*, *C44*(3), 231–274.

Avérous, L., Fringant, C., & Moro, L. (2001). Plasticized starch–cellulose interactions in polysaccharide composites. *Polymer*, *42*(15), 6565–6572.

Bharadwaj, R. K. (2001). Modeling the barrier properties of polymer-layered silicate nanocomposites. *Macromolecules*, *34*(26), 9189–9192.

Bordes, P., Pollet, E., & Avérous, L. (2009). Nano-biocomposites: Biodegradable polyester/nanoclay systems. *Progress in Polymer Science*, *34*(2), 125–155.

Chivrac, F., Pollet, E., & Avérous, L. (2009). Progress in nano-biocomposites based on polysaccharides and nanoclays. *Materials Science & Engineering R-Reports*, *67*(1), 1–17.

Chivrac, F., Pollet, E., Dole, P., & Avérous, L. (2010). Starch-based nano-biocomposites: Plasticizer impact on the montmorillonite exfoliation process. *Carbohydrate Polymers*, *79*(4), 941–947.

Chivrac, F., Pollet, E., Schmutz, M., & Avérous, L. (2008). New approach to elaborate exfoliated starch-based nanobiocomposites. *Biomacromolecules*, *9*(3), 896–900.

Cyras, V. P., Manfredi, L. B., Ton-That, M. T., & Vazquez, A. (2008). Physical and mechanical properties of thermoplastic starch/montmorillonite nanocomposite films. *Carbohydrate Polymers*, *73*(1), 55–63.

Enrione, J. I., Hill, S. E., & Mitchell, J. R. (2007). Sorption behavior of mixtures of glycerol and starch. *Journal of Agricultural and Food Chemistry*, *55*(8), 2956–2963.

Gaudin, S., Lourdin, D., Forssell, P. M., & Colonna, P. (2000). Antiplasticisation and oxygen permeability of starch-sorbitol films. *Carbohydrate Polymers*, *43*(1), 33–37.

Gill, E., Murra, W., & Wright, M. (1981). *Practical optimization* (p. 401). London: Academic Press.

Gontard, N. (1991). *Films et enrobages comestibles: étude et amélioration des propriétés filmogènes du gluten de blé*. PhD Thesis Univ. Montpellier II, Montpellier, France.

Gorrasi, G., Tortora, M., Vittoria, V., Pollet, E., Lepoittevin, B., Alexandre, M., et al. (2003). Vapor barrier properties of polycaprolactone montmorillonite nanocomposites: Effect of clay dispersion. *Polymer*, *44*(8), 2271–2279.

Guillard, V., Broyart, B., Bonazzi, C., Guilbert, S., & Gontard, N. (2003). Moisture diffusivity in sponge cake as related to porous structure evaluation and moisture content. *Journal of Food Science*, *68*(2), 555–562.

Hanson, T., Cramer, W., Abraham, W., & Lancaster, E. (1971). Rates of water-vapor absorption in granular corn starch. *Chemical Engineering Progress Symposium Series*, *108*(71), 35–42.

Karathanos, V., Villalobos, G., & Saravacos, G. (1990). Comparison of two methods of estimation of the effective diffusivity from drying data. *Journal of Food Science*, *55*, 218–231.

Katz, J. (1930). Uber die Anderungen im Röntgenspektrum der Stärke beim Backen und beim Altackenwerden des Brotes. *Zeitschrift für Physikalische Chemie*, *150*, 37–59.

Labuza, T. P. (1968). Sorption phenomena in foods. *Food Technology*, *22*, 15–24.

Lourdin, D., Coignard, L., Bizot, H., & Colonna, P. (1997). Influence of equilibrium relative humidity and plasticizer concentration on the water content and glass transition of starch materials. *Polymer*, *38*(21), 5401–5406.

Mali, S., Grossmann, M. V. E., Garcia, M. A., Martino, M. N., & Zaritzky, N. E. (2006). Effects of controlled storage on thermal, mechanical and barrier properties of plasticized films from different starch sources. *Journal of Food Engineering*, *75*(4), 453–460.

McHugh, T. H., Avenabustillos, R., & Krochta, J. M. (1993). Hydrophilic edible films—Modified procedure for water-vapor permeability and explanation of thickness effects. *Journal of Food Science*, *58*(4), 899–903.

Mondragon, M., Mancilla, J. E., & Rodriguez-Gonzalez, F. J. (2008). Nanocomposites from plasticized high-amylopectin, normal and high-amylose maize starches. *Polymer Engineering and Science*, *48*(7), 1261–1267.

Park, H. M., Lee, W. K., Park, C. Y., Cho, W. J., & Ha, C. S. (2003). Environmentally friendly polymer hybrids. Part I. Mechanical, thermal, and barrier properties of thermoplastic starch/clay nanocomposites. *Journal of Materials Science*, *38*(5), 909–915.

Phan, T. D., Debeaufort, F., Luu, D., & Voilley, A. (2005). Functional properties of edible agar-based and starch-based films for food quality preservation. *Journal of Agricultural and Food Chemistry*, *53*(4), 973–981.

Ray, S. S., & Okamoto, M. (2003). Polymer/layered silicate nanocomposites: A review from preparation to processing. *Progress in Polymer Science*, *28*(11), 1539–1641.

Rindlav-Westling, A., Stading, M., Hermansson, A. M., & Gatenholm, P. (1998). Structure, mechanical and barrier properties of amylose and amylopectin films. *Carbohydrate Polymers*, *36*(2–3), 217–224.

Roca, E., Broyart, B., Guillard, V., Guilbert, S., & Gontard, N. (2007). Controlling moisture transport in a cereal porous product by modification of structural or formulation parameters. *Food Research International*, *40*(4), 461–469.

Roca, E., Guillard, V., Broyart, B., Guilbert, S., & Gontard, N. (2008). Effective moisture diffusivity modelling versus food structure and hygroscopicity. *Food Chemistry*, *106*(4), 1428–1437.

Sorrentino, A., Gorrasi, G., & Vittoria, V. (2007). Potential perspectives of bio-nanocomposites for food packaging applications. *Trends in Food Science & Technology*, *18*(2), 84–95.

Swanson, C. L., Shogren, R. L., Fanta, G. F., & Imam, S. H. (1993). Starch–plastic materials—Preparation, physical properties, and biodegradability (a review of recent USDA research). *Journal of Environmental Polymer Degradation*, *1*(2), 155–166.

Tang, X. Z., Alavi, S., & Herald, T. J. (2008a). Barrier and mechanical properties of starch-clay nanocomposite films. *Cereal Chemistry*, *85*(3), 433–439.

Tang, X. Z., Alavi, S., & Herald, T. J. (2008b). Effects of plasticizers on the structure and properties of starch-clay nanocomposite films. *Carbohydrate Polymers*, *74*(3), 552–558.

Tomka, I. (1991). Thermoplastic starch. *Advances in Experimental Medicine and Biology*, *302*, 627–637.

Van Soest, J. J. G., De Wit, D., Tournois, H., & Vliegenthart, J. F. G. (1994). The influence of glycerol on structural-changes in waxy maize starch as studied by Fourier-transform infrared-spectroscopy. *Polymer*, *35*(22), 4722–4727.

Van Soest, J., Hulleman, S., De Wit, D., & Vliegenthart, J. (1996a). Changes in the mechanical properties of thermoplastic potato starch in relation with changes in B-type crystallinity. *Carbohydrate Polymer*, *29*(3), 225–232.

Van Soest, J., Hulleman, S., De Wit, D., & Vliegenthart, J. (1996b). Crystallinity in starch bioplastics. *Industrial Crops and Products*, *5*(1), 11–22.

Van Soest, J. J. G., & Knooren, N. (1997). Influence of glycerol and water content on the structure and properties of extruded starch plastic sheets during aging. *Journal of Applied Polymer Science*, *64*(7), 1411–1422.

Yu, X., Schmidt, A. R., Bello-Perez, L. A., & Schmidt, S. J. (2008). Determination of the bulk moisture diffusion coefficient for corn starch using an automated water sorption instrument. *Journal of Agricultural and Food Chemistry*, *56*(1), 50–58.

Zeppa, C., Gouanve, F., & Espuche, E. (2009). Effect of a plasticizer on the structure of biodegradable starch/clay nanocomposites: Thermal, water-sorption, and oxygen-barrier properties. *Journal of Applied Polymer Science*, *112*(4), 2044–2056.

Zhang, Y., & Han, J. H. (2008). Sorption isotherm and plasticization effect of moisture and plasticizers in pea starch film. *Journal of Food Science*, *73*(7), E313–E324.